

Density functional for short-range correlation: Accuracy of the random-phase approximation for isoelectronic energy changes

Zidan Yan, John P. Perdew, and Stefan Kurth*

Department of Physics and Quantum Theory Group, Tulane University, New Orleans, Louisiana 70118

(Received 7 December 1999)

Within a density-functional context, the random-phase approximation (RPA) for the correlation energy makes a short-range error that is well suited for correction by a local spin density or generalized-gradient approximation (GGA). Here we construct a GGA for the short-range correction, following the same reliable procedure used earlier to construct the GGA for the whole exchange-correlation energy: real-space cutoff of the spurious long-range contribution to the gradient expansion of the hole around an electron. The resulting density functional is nearly local and predicts a substantial correction to the RPA correlation energy of an atom but very small corrections to the RPA atomization energy of a molecule, which may by itself come close to “chemical accuracy” and to the RPA surface energy of a metal. A by-product of this work is a density functional for the system-averaged correlation hole within RPA.

I. INTRODUCTION

Density-functional theory^{1,2} is widely used for electronic structure calculations in solid-state physics and quantum chemistry. Approximations (e.g., Ref. 3) for the exchange-correlation energy as explicit functionals of the electron density may be approaching a limit of accuracy. Further accuracy can be achieved by using the Kohn-Sham one-electron orbitals, which are implicit functionals of the density. Many directions are being explored, e.g., Refs. 4–12. Here we shall discuss one we call RPA+, in which only the short-range part of the correlation energy is represented by an explicit density functional.¹³

The random-phase approximation (RPA) of Pines^{14–16} gives the simplest finite estimate for the correlation energy per particle of the uniform electron gas, and finds a natural extension^{13,17,18} to inhomogeneous systems within the Kohn-Sham density-functional theory.^{1,2} The RPA (using Kohn-Sham and not Hartree orbitals) is exact for exchange and long-range correlation^{17,18} but a poor approximation for short-range correlation. For the uniform electron gas at metallic densities, the RPA on-top correlation hole is much too deep,¹⁹ making the correlation energy much too negative. The short-range correction to the correlation energy for this system is, however, only weakly dependent upon the density parameter $r_s = (3/4\pi n)^{1/3}$ and relative spin polarization $\zeta = (n_\uparrow - n_\downarrow)/n$ (see Figs. 13 and 14 of Ref. 20), and tends as $r_s \rightarrow 0$ to the “second-order exchange” energy, +0.024 hartree/electron, independent of ζ .

While the short-range correction is a major part of the total correlation energy, it could make a much smaller contribution to isoelectronic (electron-number-conserving) energy differences. For example, the RPA spin susceptibility of the uniform gas (Table V of Ref. 21) is very close to the true spin susceptibility, and even diverges at a density ($r_s \approx 20$) close to that at which a recent quantum Monte Carlo calculation²² found a magnetic transition (see also Ref. 23). The RPA also predicts a metal-insulator transition,²⁴ possibly a Wigner crystallization, at a density ($r_s \approx 60$) close to that

found in the Monte Carlo calculation. Another example is the second-order coefficient $C_c(n)$ in the gradient expansion

$$E_c[n] = \int d^3r [n \epsilon_c^{unif}(n) + C_c(n) |\nabla n|^2 / n^{4/3} + \dots] \quad (1)$$

of the correlation energy for a slowly varying density $n(\mathbf{r})$. The RPA value for $C_c(n)$ is exact in the high-density limit, and applicable^{18,25} at metallic densities; this coefficient is derived isoelectronically by imposing a long-wavelength density oscillation upon the uniform gas.

Recently, RPA calculations have been performed for self-consistent jellium surfaces.^{26–28} We have argued from several perspectives^{13,29} that the short-range correction to the RPA surface energy may be only a few percent of the surface exchange-correlation energy. RPA calculations have been performed for jellium clusters,^{30–32} and those for bulk crystalline solids are on the horizon.^{33,34} We are not aware of RPA calculations for the energies of atoms and molecules, but such calculations may be feasible by simplification³⁵ of a coupled-cluster code³⁶ or modification³⁷ of a second-order Moeller-Plesset code.³⁸

In previous work, Kurth and Perdew¹³ constructed a generalized-gradient approximation for the short-range correlation energy of an inhomogeneous system, and suggested that its use together with RPA might achieve chemical accuracy (molecular atomization energies correct to 1 kcal/mol = 0.0434 eV/molecule). In this work, by a more reliable construction of the GGA, we suggest that RPA by itself may come close to chemical accuracy, since the revised corrections are very small. We still follow the basic idea of Ref. 13: Local-spin-density^{1,2} (LSD) and generalized gradient approximations^{3,39,40} (GGA) are most accurate for the short-range part of the exchange-correlation energy^{17,41} but fail in the long-range limit. Therefore, an accurate functional can be constructed by combining RPA with the short-range piece of LSD or GGA correlation.⁴²

Kurth and Perdew defined the short-range correlation energy as

$$E_{c,sr} = E_{xc} - E_{xc}^{RPA} = E_c - E_c^{RPA}, \quad (2)$$

and then used either GGA or LSD to approximate this energy, e.g.,

$$E_{c,sr}^{GGA} = E_c^{GGA} - E_c^{GGARPA}, \quad (3)$$

where E_c^{GGA} and E_c^{GGARPA} are the correlation energies evaluated in GGA beyond and within RPA, respectively.

The approximation for E_{xc} , which we sometimes call RPA+, is

$$E_{xc}^{RPA+} = E_{xc}^{RPA} + (E_{xc}^{GGA} - E_{xc}^{GGARPA}). \quad (4)$$

In Eq. (4), $E_{c,sr}^{GGA} = E_{xc}^{GGA} - E_{xc}^{GGARPA}$ provides a short-range correction to RPA. But we can also write

$$E_{xc}^{RPA+} = E_{xc}^{GGA} + (E_{xc}^{RPA} - E_{xc}^{GGARPA}), \quad (5)$$

in which $E_{xc}^{RPA} - E_{xc}^{GGARPA}$ provides a long-range correction to GGA exchange and correlation. Here the range is that of the interelectronic separation u defined later.

For the GGA correlation energy, Kurth and Perdew used the analytic form proposed by Perdew, Burke, and Ernzerhof,³ (PBE)

$$E_c^{GGA}[n_\uparrow, n_\downarrow] = \int d^3r n(\mathbf{r}) [\epsilon_c^{unif}(r_s, \zeta) + H(r_s, \zeta, t, \epsilon_c^{unif}(r_s, \zeta))], \quad (6)$$

where r_s is the local Wigner-Seitz radius [$n = 3/(4\pi r_s^3) = k_F^3/(3\pi^2)$], $\zeta = (n_\uparrow - n_\downarrow)/n$, where $n = n_\uparrow + n_\downarrow$ is the total electron density, and $\epsilon_c^{unif}(r_s, \zeta) < 0$ is the correlation energy per particle of a uniform electron gas.²¹ Here $t = |\nabla n|/(2\phi k_s n)$ is a dimensionless density gradient. $k_s = \sqrt{4k_F/\pi}$ is the Thomas-Fermi screening wave number, and $\phi = [(1 + \zeta)^{2/3} + (1 - \zeta)^{2/3}]/2$. (We use atomic units in which $\hbar = m = e^2 = 1$.)

The nonempirical PBE GGA of Eq. (6) was constructed to satisfy known exact conditions, and was based largely upon a numerical real-space cutoff of the spurious long-range part of the second-order gradient expansion for the correlation hole,⁴³ beyond RPA. Both RPA and beyond-RPA versions of ϵ_c^{unif} can be readily found in Ref. 21, and the beyond-RPA version of H in Ref. 43. For the RPA version of H , Kurth and Perdew used the same analytic form of H as beyond RPA, changing only the input ϵ_c^{unif} . Recently we have found that this expression for H is not appropriate in RPA. In this work, we will construct the RPA version of H by fitting it to the RPA numerical GGA results. We will then apply the new analytic short-range correlation functional to atoms, molecules, and jellium surfaces as in Ref. 13.

II. REAL-SPACE CUTOFF CONSTRUCTION OF A GGA FOR THE SHORT-RANGE CORRELATION ENERGY

The exchange-correlation energy may be written^{17,18} as an integral over interelectronic separations \mathbf{u} :

$$E_{xc} = \frac{1}{2} \int d^3r \int d^3u \frac{n(\mathbf{r})n_{xc}(\mathbf{r}, \mathbf{r} + \mathbf{u})}{u}. \quad (7)$$

Here $n_{xc}(\mathbf{r}, \mathbf{r} + \mathbf{u})$ is the density at $\mathbf{r} + \mathbf{u}$ of the exchange-correlation hole about an electron at \mathbf{r} , defined as

$$\begin{aligned} n_{xc}(\mathbf{r}, \mathbf{r} + \mathbf{u}) &= \int_0^1 d\lambda n_\lambda^\lambda(\mathbf{r}, \mathbf{r} + \mathbf{u}) \\ &= \int_0^1 d\lambda [\langle \Psi_\lambda | \hat{\delta}n(\mathbf{r}) \hat{\delta}n(\mathbf{r} + \mathbf{u}) | \Psi_\lambda \rangle / n(\mathbf{r}) - \delta(\mathbf{u})], \end{aligned} \quad (8)$$

where $\hat{\delta}n(\mathbf{r}) = \hat{n}(\mathbf{r}) - n(\mathbf{r})$ is the density fluctuation operator. The integral over λ is a coupling-constant integration, in which Ψ_λ is the ground state of the Hamiltonian with electron-electron repulsion λ/u , and with external potential $v_\lambda(\mathbf{r})$ adjusted to keep $\langle \Psi_\lambda | \hat{n}(\mathbf{r}) | \Psi_\lambda \rangle = n(\mathbf{r})$ fixed at the physical or $\lambda = 1$ density. At $\lambda = 0$, the system reduces to the Kohn-Sham noninteracting reference, the correlation is completely turned off, and the exchange-correlation hole becomes the exchange hole $n_x = n_{xc}^{\lambda=0}$. The correlation hole is defined as $n_c = n_{xc} - n_x$, and the correlation energy E_c is related to the correlation hole by

$$E_c = \frac{1}{2} \int d^3r \int d^3u \frac{n(\mathbf{r})n_c(\mathbf{r}, \mathbf{r} + \mathbf{u})}{u}. \quad (9)$$

These holes satisfy the following exact conditions:

$$n_x(\mathbf{r}, \mathbf{r} + \mathbf{u}) \leq 0, \quad (10)$$

$$\int d^3u n_x(\mathbf{r}, \mathbf{r} + \mathbf{u}) = -1, \quad (11)$$

and

$$\int d^3u n_c(\mathbf{r}, \mathbf{r} + \mathbf{u}) = 0, \quad (12)$$

both beyond and within RPA (or other approximations based upon the Dyson equation; see Appendix A). The LSD is a rather reliable approximation, because the LSD hole is the hole for a possible physical system (the uniform electron gas) and thus satisfies all the above exact conditions. In an effort to improve upon LSD, one can expand the energy in a gradient expansion, and include the $|\nabla n|^2$ term. However, this gradient expansion approximation (GEA) often does worse than LSD,^{18,44} because the corresponding hole is not the hole of any physical system, and so violates the exact conditions Eqs. (10)–(12).

Perdew, Burke, and Wang⁴³ proposed a real-space cutoff procedure to overcome this problem, by removing unphysical long-range contributions to the GEA hole, thereby restoring Eqs. (10)–(12). This procedure defines a numerical GGA that retains the good features of LSD, while improving the description of the average hole (and therefore the energy) by including the density gradient.

The spherically averaged and coupling-constant averaged numerical GGA correlation hole is⁴³

$$\begin{aligned} n_c^{GGA}(r_s, \zeta, t, v) &= \phi^5 k_s^2 [A_c(r_s, \zeta, v) \\ &\quad + t^2 B_c(r_s, \zeta, v)] \theta(v_c - v), \end{aligned} \quad (13)$$

where A_c is the local term, and B_c the second order gradient correction. v is a reduced separation on the Thomas-Fermi screening-length scale, $v = \phi k_s u$, and $v_c(r_s, \zeta, t)$ is the upper limit satisfying the sum rule

$$\int_0^{v_c} dv 4\pi v^2 [A_c(r_s, \zeta, v) + t^2 B_c(r_s, \zeta, v)] = 0. \quad (14)$$

Once we use Eq. (14) to find v_c , we can calculate the GGA correlation energy per electron

$$\epsilon_c^{GGA}(r_s, \zeta, t) = \phi^3 \int_0^{v_c} dv \frac{4\pi v^2}{2v} [A_c(r_s, \zeta, v) + t^2 B_c(r_s, \zeta, v)], \quad (15)$$

or the gradient correction term H

$$H(r_s, \zeta, t) = \epsilon_c^{GGA}(r_s, \zeta, t) - \epsilon_c^{unif}(r_s, \zeta). \quad (16)$$

The local term A_c consists of a long-range part \bar{f}_1 and a short-range part \bar{f}_2 :

$$A_c(r_s, \zeta, v) = [\bar{f}_1(v) + \bar{f}_2(r_s, \zeta, v)]/4\pi v^2. \quad (17)$$

The beyond-RPA expressions for \bar{f}_1 and \bar{f}_2 can be found in Ref. 45, and that for B_c in Ref. 43. For the RPA version, the expressions for \bar{f}_1 and B_c are unchanged. Since within RPA the on-top ($u=0$) correlation hole of the uniform electron gas and the corresponding cusp condition are different from those beyond RPA, we need to modify the expression for the short-range part \bar{f}_2 :

$$\bar{f}_2(v) = [-a_1 - (a_2 - a_1 b_1)v + c_1 v^2 + c_2 v^3 + c_3 v^4 + c_4 v^5] \exp[-d(\zeta)(k_F u / \phi)^2], \quad (18)$$

where the coefficients $\{c_i\}$ are functions of r_s and ζ , given by Eqs. (38), (39), (43), and (44) of Ref. 45. In Eq. (18), only these four coefficients need to be modified. For c_3 and c_4 , we can still use their beyond-RPA analytic forms, but now use the RPA version of ϵ_c^{unif} as the input. The other two coefficients, c_1 and c_2 , which are chosen to reproduce the value of the pair distribution function of the uniform electron gas at zero separation $u=0$ and its corresponding cusp condition, respectively, require new expressions.

The pair distribution function $g_\lambda(\mathbf{r}, \mathbf{r} + \mathbf{u})$ is related to the exchange-correlation hole at coupling strength λ ,

$$n_{xc}^\lambda(\mathbf{r}, \mathbf{r} + \mathbf{u}) = n(\mathbf{r} + \mathbf{u}) [g_\lambda(\mathbf{r}, \mathbf{r} + \mathbf{u}) - 1]. \quad (19)$$

The exchange part of $g_\lambda - 1$ is

$$g_x(\mathbf{r}, \mathbf{r} + \mathbf{u}) - 1 = g_{\lambda=0}(\mathbf{r}, \mathbf{r} + \mathbf{u}) - 1, \quad (20)$$

and the rest is correlation. We define $g = g_{\lambda=1}$, and the coupling-constant average \bar{g} . For the uniform electron gas with density parameter r_s ,⁴⁵

$$g^{unif}(r_s, \zeta, u) = (1 + r_s \partial / \partial r_s) \bar{g}^{unif}(r_s, \zeta, u). \quad (21)$$

As in Ref. 45, we model \bar{g}^{unif} and then find g^{unif} from Eq. (21). The cusp condition on $g_\lambda^{unif}(r_s, \zeta, u)$ beyond RPA is^{46,47}

$$\left. \frac{dg_\lambda^{unif}}{du} \right|_{u=0} = \lambda g_\lambda^{unif} \Big|_{u=0}. \quad (22)$$

Within RPA,⁴⁸ the cusp condition on $g_\lambda^{unif}(r_s, \zeta, u)$ is

$$\left. \frac{dg_\lambda^{unif,RPA}}{du} \right|_{u=0} = \lambda, \quad (23)$$

whence $d\bar{g}^{unif,RPA}/du|_{u=0} = 1/2$. Note that Eq. (23) holds for arbitrary spin polarization. The proof of this statement is sketched in Appendix B. By applying the RPA on-top pair distribution function for the uniform electron gas and the corresponding cusp condition (see Appendix B for detailed expressions), we obtain within RPA

$$c_1 = -0.0012529 + 0.1244p + \frac{0.61386}{\phi^5 r_s^2} [2\bar{g}_c^{unif,RPA}(r_s, \zeta, u=0)] \quad (24)$$

and

$$c_2 = 0.0033894 - 0.054388p + \frac{0.39270}{\phi^6 r_s^{3/2}}, \quad (25)$$

where

$$\begin{aligned} \bar{g}_c^{unif,RPA}(r_s, \zeta, u=0) &= \bar{g}_c^{unif,RPA}(r_s, \zeta=0, u=0) \\ &+ \zeta^2 [\bar{g}_c^{unif,RPA}(r_s, \zeta=1, u=0) \\ &- \bar{g}_c^{unif,RPA}(r_s, \zeta=0, u=0)], \end{aligned} \quad (26)$$

is our assumed ζ dependence (similar to that beyond RPA) for the correlation contribution to the RPA pair distribution function at zero separation for the uniform electron gas. The $\zeta=0$ and $\zeta=1$ limits for $\bar{g}_c^{unif,RPA}(r_s, \zeta, u=0)$ are presented in Appendix B. The other symbols are the same as those in the beyond-RPA version [Eqs. (38) and (39) of Ref. 45].

Figures 1 and 2 show the RPA analogs of Figs. 3 and Fig. 6 of Ref. 45 for the uniform-gas pair distribution function g^{unif} and its coupling-constant average \bar{g}^{unif} . We evaluate \bar{g}^{unif} by using the new c_1, c_2, c_3, c_4 and then obtain g^{unif} from Eq. (21). The accurate match of the analytic g^{unif} curve to the numerical RPA g^{unif} curve (from Appendix B) indicates that our analytic model for \bar{g}^{unif} has been properly constructed.

Figures 3 and 4 show our analytic model for the correlation contribution to the coupling-constant average of the pair distribution function divided by the density parameter, $\bar{g}_c^{RPA,unif}/r_s$, as a function of u/r_s , for the spin-unpolarized and polarized uniform gas. Figs. 7 and 8 of Ref. 49 provide the exact RPA results. By comparing our analytic results with the exact ones, we can see that the analytic model of Ref. 45, which was originally designed for the beyond-RPA uniform gas, with a minor change of its coefficients, is also a very accurate representation for the RPA uniform gas, for a wide range of density parameters r_s .

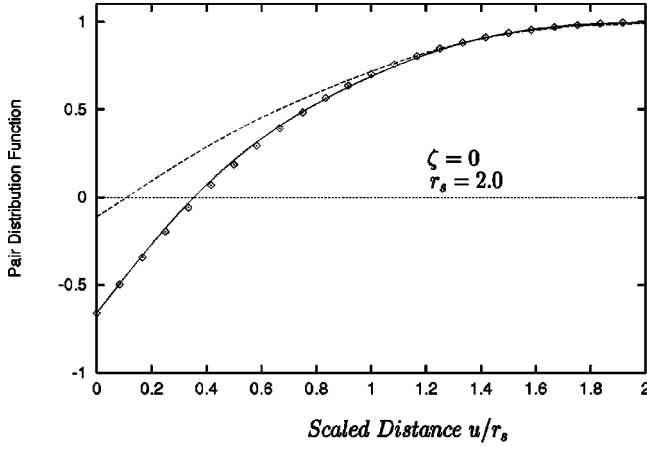


FIG. 1. Our analytic model for the nonoscillatory part of the RPA pair distribution function g (solid curve) and its coupling-constant average \bar{g} (dashed curve), for a uniform electron gas with density parameter $r_s=2$ in the spin-unpolarized case ($\zeta=0$). Also shown are the exact numerical results (diamonds) from Eq. (B4). (For the analogous figure beyond RPA, see Fig. 3 of Ref. 45.) Our analytic model is similarly accurate for $r_s=5$ and $r_s=10$.

Figures 5 and 6 show the short-range correlation contribution to the coupling-constant average of the pair distribution function divided by the density parameter, $\bar{g}_{c,sr}^{unif}/r_s$, as a function of u/r_s , for the spin-unpolarized and polarized uniform gas. $\bar{g}_{c,sr}^{unif}/r_s$ is truly short-ranged, without the positive u^{-4} long-range tail of \bar{g}_c^{unif}/r_s . With RPA and beyond-RPA versions of the gradient expansion for the correlation hole well defined, we can proceed to the numerical GGA calculation: First we use Eq. (14) to find the cutoff v_c , then use this v_c in Eq. (13) to find n_c , and finally Eq. (15) to find ϵ_c or Eq. (16) to find H .

By fitting to the numerical GGA results, we obtain the RPA version of H ,

$$H^{RPA} = \gamma \phi^3 \times \ln \left[1 + \frac{\beta}{\gamma} t^2 \left(\frac{1 + \xi_1 A_{RPA} t^2 + A_{RPA}^2 t^4}{1 + \xi_1 A_{RPA} t^2 + \xi_2 A_{RPA}^2 t^4 + A_{RPA}^3 t^6} \right) \right], \quad (27)$$

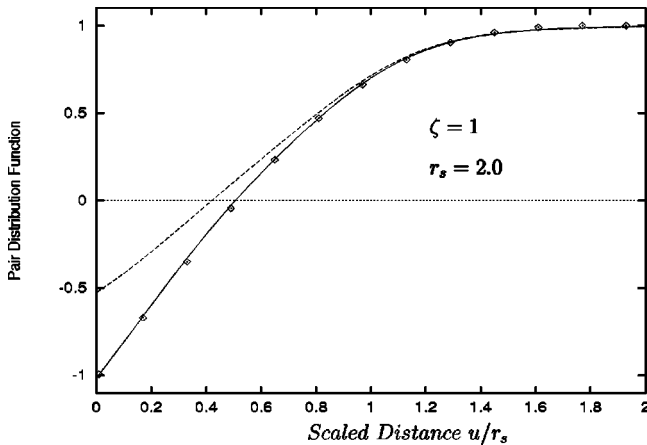


FIG. 2. Same as Fig. 1, but for $\zeta=1$.

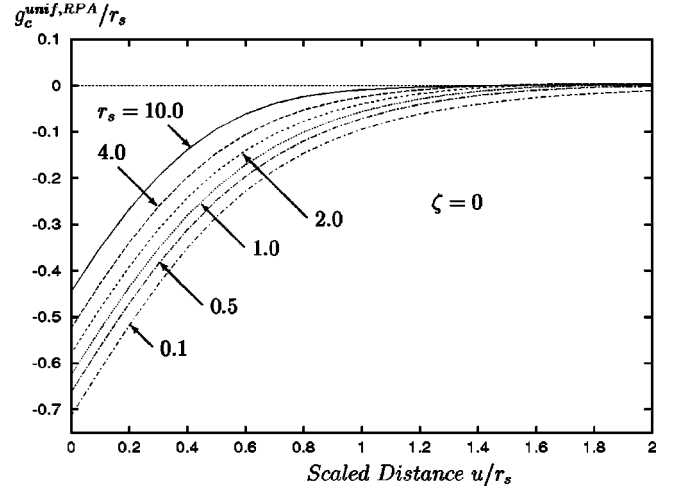


FIG. 3. Our analytic model for the RPA correlation contribution to the pair distribution function of an unpolarized ($\zeta=0$) uniform electron gas divided by the density parameter r_s , $g_c^{unif,RPA}/r_s$, as a function of u/r_s . For the exact numerical results of Eq. (B4), see Fig. 7 of Ref. 49.

where

$$\xi_1 = 3.8 + 2.0[\phi(k_s/k_F)t - 2.17]\zeta^4, \quad (28)$$

$$\xi_2 = 6.2 + 9.0\zeta^4, \quad (29)$$

and

$$A_{RPA} = \frac{\beta}{\gamma} [\exp(-\epsilon_c^{unif,RPA}/\gamma\phi^3) - 1]^{-1}. \quad (30)$$

These are the RPA analogs of Eqs. (7) and (8) of Ref. 3.

Figure 7 shows both the numerical and analytic short-range correlation energies per electron $\epsilon_{c,sr}^{GGA}$ versus the alternative reduced gradient $s = |\nabla n|/2k_F n = \phi(k_s/k_F)t$ for the spin-unpolarized case $\zeta=0$. For energetically important regions of most physical systems, s ranges from 0 to 3. This figure is the analog of Fig. 1(b) of Ref. 13. Compared with that figure, the new curves are flatter, i.e., the new H^{RPA} results in a more local short-range correlation. Figures 8 and 9 are the same as Fig. 7, but for $\zeta=0.5$ and $\zeta=1$, respec-

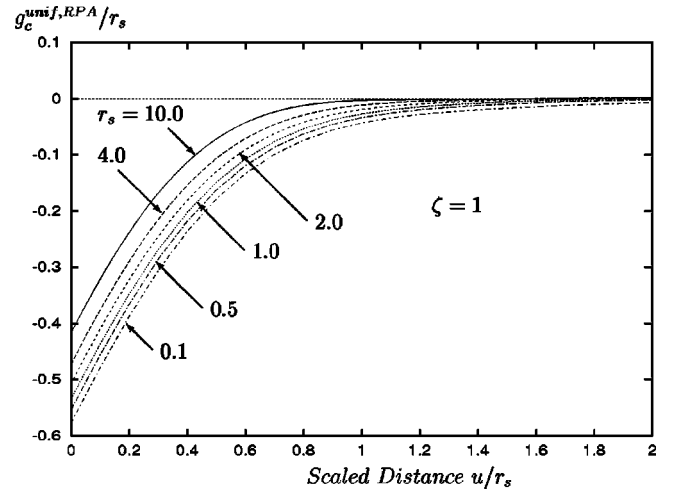


FIG. 4. Same as Fig. 3, but for $\zeta=1.0$.

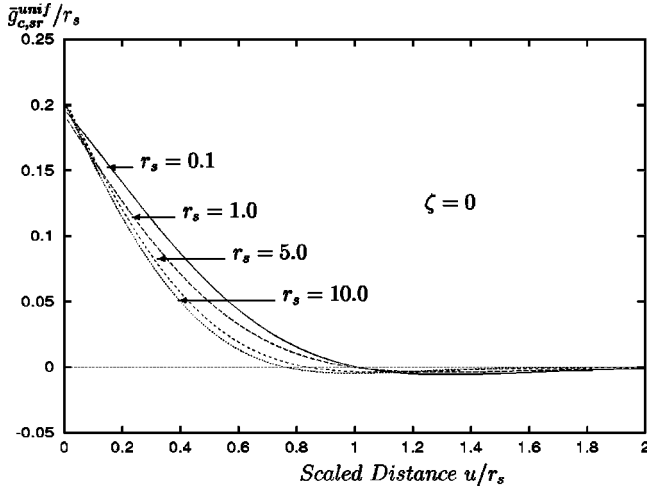


FIG. 5. The short-range correlation contribution to the average over coupling constant of the pair distribution function for the unpolarized ($\zeta=0$) uniform electron gas divided by the density parameter r_s , $\bar{g}_{c,sr}^{unif}/r_s$, as a function of u/r_s .

tively. Note that our Eq. (27) is not the result of a direct fit to the numerical H^{RPA} , but rather a fit to the numerical $\epsilon_{c,sr}^{GGA} = (\epsilon_c^{unif} + H) - (\epsilon_c^{unif,RPA} + H^{RPA})$.

Kurth and Perdew¹³ calculated the total and short-range correlation energies for various atoms using LSD and GGA. They found that the short-range correlation energy has a density functional that is rather local, and we find it even more local.

Görling and Levy⁵⁰ showed that, under a uniform scaling of the density $n(\mathbf{r}) \rightarrow n_\gamma(\mathbf{r}) = \gamma^3 n(\gamma\mathbf{r})$, the correlation energy of a finite system scales to a finite value as $\gamma \rightarrow \infty$, i.e.,

$$\lim_{\gamma \rightarrow \infty} E_c[n_\gamma] = E_c^{(2)}[n], \quad (31)$$

where $E_c^{(2)}$ is the second-order energy of Görling and Levy perturbation theory (GL2). Kurth and Perdew used Eq. (9) of Ref. 3 to evaluate this energy. Since we now use a new RPA H , the analog of Eq. (9) of Ref. 3 becomes

$$E_c^{(2),RPA} = \int d^3r n(\mathbf{r}) \gamma \phi^3 \ln \left[Z \left(\frac{1 + \xi_1 Z + Z^2}{1 + \xi_1 Z + \xi_2 Z^2 + Z^3} \right) \right] \quad (32)$$

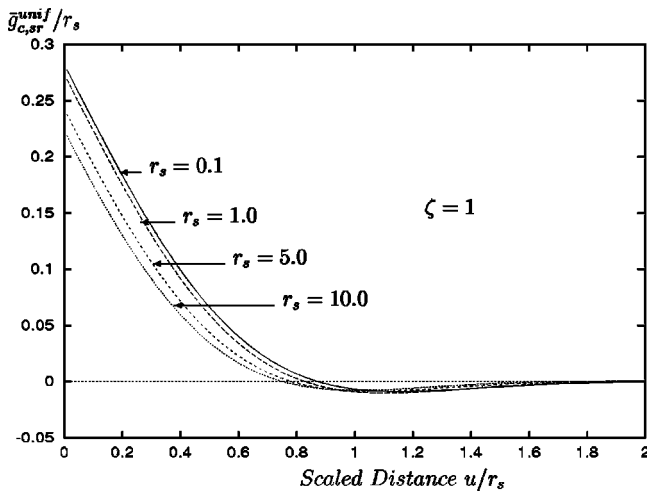


FIG. 6. Same as Fig. 5, but for $\zeta=1.0$.

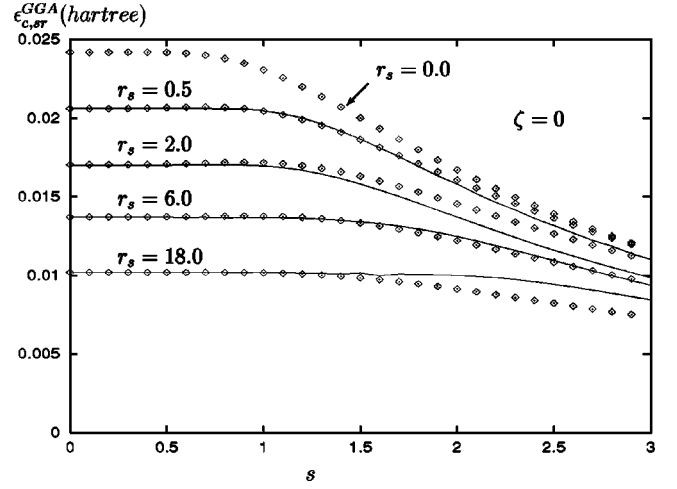


FIG. 7. GGA short-range correlation energy per particle, $\epsilon_{c,sr}^{GGA} = \epsilon_c^{GGA} - \epsilon_c^{GGARPA}$, as a function of the dimensionless reduced density gradient $s = |\nabla n|/(2k_F n)$, for the unpolarized case ($\zeta=0$). s measures how fast the density varies on the scale of the local Fermi wavelength. The $s \rightarrow 0$ limit is $\epsilon_{c,sr}^{LSD}$. The solid curves are from the real-space cutoff procedure, while the diamonds are from the analytic expressions. Compare with Fig. 1(b) of Ref. 13.

where $Z = \chi s^2 / \phi^2$. The definitions of all the other symbols are the same as in Eq. (9) of Ref. 3, except that in RPA ω has a dependence on ζ : $\omega = 0.046644 + 0.024179/\phi^3$.

III. NUMERICAL RESULTS FOR ATOMS, MOLECULES, AND JELLIUM SURFACES

Our refined results for the short-range correlation energies of atoms in GGA and GGA GL2 are presented in Table I. Compared to the old results,¹³ the present results are more local, in agreement with what we observed in Fig. 7.

For an accurate description of chemical processes, a precise determination of molecular atomization energies is very important. Table II displays our new results for the short-range correlation contribution $\Delta_{c,sr}$ to the atomization energy Δ of some small molecules in GGA and GGA GL2. The new GGA short-range contributions are significantly smaller in magnitude than the old ones. The smallness of this

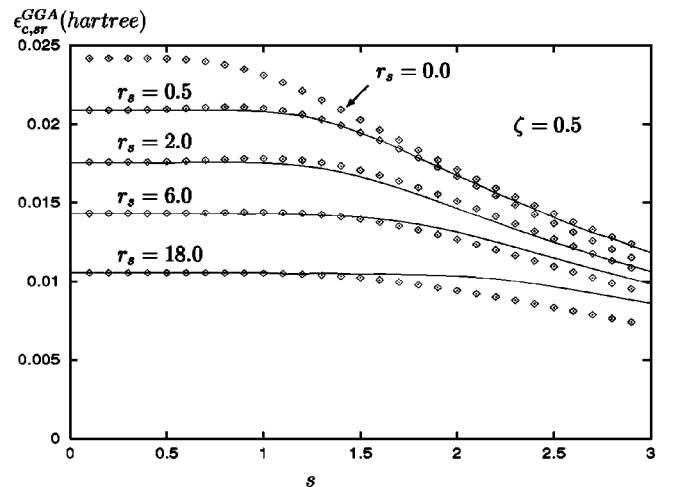
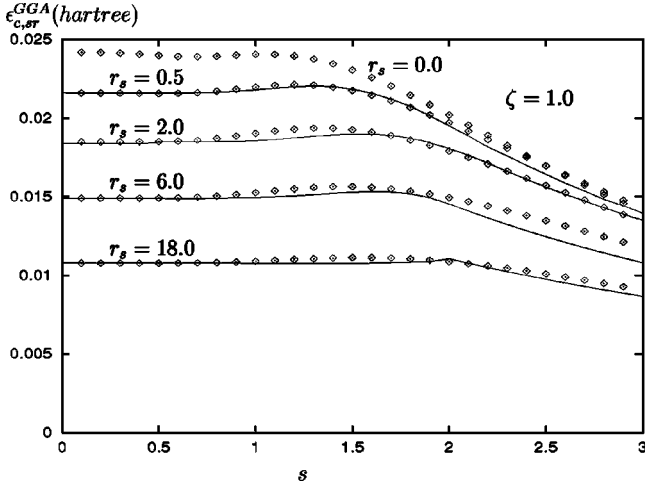


FIG. 8. Same as Fig. 7, but for $\zeta=0.5$.

FIG. 9. Same as Fig. 7, but for $\zeta = 1.0$.

quantity suggests that RPA [or better, RPA+ of Eq. (4)] can accurately predict atomization energies of molecules. The short-range contributions in GL2 are somewhat larger than those beyond GL2. But in fact, second-order perturbation theory, which works reasonably well for the total correlation energy of an atom, is not nearly good enough for atomization energies of molecules.⁵¹

Jellium is a useful model for simple metals. In Ref. 13, Kurth and Perdew estimated jellium surface exchange-correlation energies by using the PBE GGA to make the short-range correction to the results of the full RPA calculation performed by Pitarke and Eguiluz.^{26,27} Their RPA+ results of Eq. (4) are extremely close to those in LSD, the

TABLE I. Short-range correlation corrections $E_{c,sr} = E_c - E_c^{RPA}$ to the RPA energies of atoms and ions in LSD and in the new GGA of the present work. Also shown is the short-range part of the Görling-Levy second-order energy, using the new GGA. All functionals were evaluated with exchange-only optimized effective potential (Ref. 58) densities. Energies in hartrees. For the hydrogen atom, the short-range correction to RPA is a self-interaction correction. For comparison, the total GGA correlation energies for He, Ne, and Xe are -0.0420 , -0.3513 , and -2.9181 hartrees, respectively.

Atom	$E_{c,sr}^{LSD}$	$E_{c,sr}^{GGA}$	$E_{c,sr}^{GGAGL2}$
H	0.0177	0.0169	0.0215
He	0.0367	0.0353	0.0427
Li ⁺	0.0392	0.0373	0.0428
Be ²⁺	0.0406	0.0383	0.0428
Li	0.0541	0.0519	0.0649
Be ⁺	0.0574	0.0549	0.0654
Be	0.0719	0.0694	0.0868
Ne ⁶⁺	0.0829	0.0790	0.0877
N	0.1361	0.1340	0.1598
Ne	0.2008	0.1984	0.2308
Ar	0.3654	0.3630	0.4216
Zn ¹²⁺	0.3929	0.3879	0.4225
Zn	0.6297	0.6293	0.7119
Kr	0.7598	0.7589	0.8569
Xe	1.1531	1.1527	1.2921

TABLE II. Short-range correlation contributions $\Delta_{c,sr}$ to the atomization energies Δ of some small molecules in LSD and in the new GGA of the present work. Also shown is the short-range part of the Görling-Levy second order energy, using the new GGA. All functionals were evaluated with self-consistent PBE GGA densities for the atoms and for the molecules at experimental geometries. The calculations were performed with a modified version of the CADPAC program (Ref. 60). Energies in kcal/mol. (1 kcal/mol = 1.594×10^{-3} hartree.) The mean atomization energy Δ for these 8 molecules is 198 kcal/mol.

Molecule	$\Delta_{c,sr}^{LSD}$	$\Delta_{c,sr}^{GGA}$	$\Delta_{c,sr}^{GGAGL2}$
H ₂	0.5	0.3	0.3
N ₂	0.1	-0.2	-1.4
O ₂	-0.7	-1.3	-2.5
F ₂	-0.5	-1.3	-2.6
CH ₄	-0.8	-2.6	-4.0
NH ₃	-0.1	-1.3	-2.6
H ₂ O	-0.4	-1.4	-2.4
HF	-0.4	-1.0	-1.4

average relative deviation being within 1%. This confirmed the accuracy of the LSD approximation for the surface energy. In the present work, we reevaluate the short-range correlation energies for the jellium surface by using the new RPA H [Eq. (27)], and combine them with the same RPA results of Refs. 26 and 27 in Table III. The new RPA+ estimates are still close to those of LSD, but are about 2% higher. The new estimates are also highly consistent with those from the latest wave-vector interpolation approach,²⁹ and those predicted by the meta-GGA functional developed by Perdew, Kurth, Zupan, and Blaha¹⁰ (PKZB). The surface exchange-correlation energies from these three approaches agree among themselves to 1%.

We have found small, *negative* short-range corrections to RPA atomization energies (Table II) and surface energies (Table III). An alternative short-range correction to RPA, the time-dependent local-density approximation (TDLDA), provides larger *positive* corrections²⁶ to jellium surface energies

TABLE III. Estimates of the jellium surface exchange-correlation energy σ_{xc} (in erg/cm²) for realistic LSD density profiles of the jellium surface. r_s is the bulk density parameter, in bohr. Shown are the results in LSD, in RPA, in TDLDA (Ref. 26), and in the RPA+ approximation of Eq. (4), which combines the RPA results of Refs. 26 and 27 with our new GGA short-range correction. (1 hartree/bohr² = 1.557×10^6 erg/cm².)

r_s	σ_{xc}^{LSD}	σ_{xc}^{RPA}	σ_{xc}^{TDLDA}	σ_{xc}^{RPA+}
2.00	3354	3467	3533	3413
2.07	2961	3064	3125	3015
2.30	2019	2098	-	2060
2.66	1188	1240	-	1214
3.00	764	801	840	781
3.28	549	579	-	563
4.00	261	278	295	268
5.00	111	119	130	113
6.00	53	58	65	54

TABLE IV. Surface exchange-correlation energies σ_{xc} (in erg/cm²) for the infinite-barrier-model density profile of the jellium surface. r_s is the bulk density parameter, in bohr. Shown are the results in LSD, in RPA (Refs. 26 and 27), and in the RPA+ approximation of Eq. (4), using our new GGA short-range correction. For analytic parametrizations of the r_s dependence within LSD and RPA+, see Eq. (26) of Ref. 59.

r_s	σ_{xc}^{LSD}	σ_{xc}^{RPA}	σ_{xc}^{RPA+}
2.07	1226	1331	1294
4.00	180	198	189
6.00	56	62	58

(Table III). However, TDLDA fails badly for the correlation energies of the uniform electron gas, where it gives about twice the needed correction to RPA.^{27,52} By construction, our RPA+ of Eq. (4) is exact for the uniform gas.

The surface energies in Table III were computed from realistic LSD electron densities for the jellium surface. Also of interest are the more rapidly varying density profiles of the infinite barrier model⁵³ (IBM). Table IV shows surface exchange-correlation energies for the IBM, evaluated in RPA (Ref. 27) and RPA+.

IV. CONCLUSIONS

In this work, by constructing a new GGA within RPA, we have improved the accuracy of the generalized-gradient approximation for the short-range correlation energy. While the RPA is not a good approximation for the total correlation energy, it seems to be a surprisingly good approximation for certain changes in correlation energy, such as those that arise in atomization or surface energies. We believe that there is a useful synergy between the RPA, which is valid for exchange and long-range correlation, and the GGA, which should be accurate for the short-range correction to RPA.

The equilibrium properties of solids (lattice constant, bulk modulus, etc.) also sample isoelectronic energy differences, and can be given accurately by the RPA. For example, the stabilized jellium model with effective valence $z^*=1$,⁵⁴ a useful zero-order model for simple metals with $1.6 \leq r_s \leq 6$, shows that the short-range correction to RPA probably expands the lattice constant by only 0.7% or less.

It may be possible⁷ to implement Kohn-Sham RPA or RPA+ [Eq. (4)] self-consistently; the resulting electron spin densities $n_\uparrow(\mathbf{r})$ and $n_\downarrow(\mathbf{r})$ are expected to be highly accurate.

Let us write the short-range correction to RPA as

$$E_{c,sr}[n_\uparrow, n_\downarrow] = \int d^3r n(\mathbf{r}) \epsilon_{c,sr}([n_\uparrow, n_\downarrow]; \mathbf{r}). \quad (33)$$

We have argued that $\epsilon_{c,sr}([n_\uparrow, n_\downarrow]; \mathbf{r})$ depends only weakly upon the spin densities n_\uparrow and n_\downarrow . For qualitative purposes, we can regard $\epsilon_{c,sr}$ as a positive constant of order 0.5 eV. Then Eq. (33) contributes *only* to those energy changes in that the electron number changes, such as ionization energies or work functions which are decreased by the amount $\epsilon_{c,sr}$ from their RPA values. The correlation potential $v_{c,\sigma}(\mathbf{r}) = \delta E_c / \delta n_\sigma(\mathbf{r})$ is shifted up by the constant $\epsilon_{c,sr}$, and the linear response kernel $\delta^2 E_{xc} / \delta n_\sigma(\mathbf{r}) \delta n_{\sigma'}(\mathbf{r}')$ is unaffected.

A by-product of our work is a density functional for the spherically and system-averaged exchange-correlation hole

$$\langle n_{xc}(u) \rangle = \frac{1}{N} \int d^3r n(\mathbf{r}) \int \frac{d\Omega_{\mathbf{u}}}{4\pi} n_{xc}(\mathbf{r}, \mathbf{r} + \mathbf{u}) \quad (34)$$

within RPA, where $N = \int d^3r n(\mathbf{r})$. A similar density functional beyond RPA was presented in Ref. 43. The RPA hole has been employed already in the wave-vector interpolation approach to the metal surface energy.²⁹

An alternative to the LSD or GGA short-range corrections to RPA is the use of an exchange-correlation kernel $f_{xc}^\lambda(\mathbf{r}, \mathbf{r}'; \omega)$, as in Ref. 52.

ACKNOWLEDGMENTS

This work was supported in part by the National Science Foundation under Grant No. DMR 98-10620, and by the Petroleum Research Fund under Grant ACS-PRF No. 33001-AC6. We thank Manfred Lein for helpful discussions, and Gerardo Ortiz for pointing out Ref. 24.

APPENDIX A: PROOF OF THE SUM RULE FOR THE EXCHANGE-CORRELATION HOLE WITHIN AND BEYOND RPA

The exchange-correlation hole can be expressed in terms of the density-density response function as¹⁸

$$n_{xc}(\mathbf{r}, \mathbf{r}') = \int_0^1 d\lambda \left(-\frac{1}{\pi n(\mathbf{r})} \int_0^\infty d\omega \text{Im}[\chi_\lambda(\mathbf{r}, \mathbf{r}')] - \delta(\mathbf{r} - \mathbf{r}') \right). \quad (A1)$$

The response function χ_λ of the interacting system is related to the Kohn-Sham response function χ_s via a Dyson-type equation⁵⁶ [see also Eq. (3) of Ref. 13] which can formally be solved for

$$\chi_\lambda(\mathbf{r}, \mathbf{r}', \omega) = \int d^3x G_\lambda^{-1}(\mathbf{r}, \mathbf{x}, \omega) \chi_s(\mathbf{x}, \mathbf{r}', \omega), \quad (A2)$$

where G_λ^{-1} is the inverse of the integral operator

$$G_\lambda(\mathbf{r}, \mathbf{r}', \omega) = \delta(\mathbf{r} - \mathbf{r}') - \int d^3x \chi_s(\mathbf{r}, \mathbf{x}, \omega) \times \left(\frac{\lambda}{|\mathbf{x} - \mathbf{r}'|} + f_{xc}^\lambda(\mathbf{x}, \mathbf{r}', \omega) \right). \quad (A3)$$

Here, $f_{xc}^\lambda(\mathbf{r}, \mathbf{r}', \omega)$ is the exchange-correlation kernel at frequency ω .⁵⁶ In the RPA, f_{xc}^λ vanishes identically.

To derive the sum rule on the exchange-correlation hole, we insert Eqs. (A2) and (A3) into Eq. (A1) and integrate

$$\begin{aligned} & \int d^3r' n_{xc}(\mathbf{r}, \mathbf{r}') \\ &= -1 - \frac{1}{\pi n(\mathbf{r})} \int_0^1 d\lambda \int d^3r' \int_0^\infty d\omega \\ & \quad \times \text{Im} \int d^3x G_\lambda^{-1}(\mathbf{r}, \mathbf{x}, \omega) \chi_s(\mathbf{x}, \mathbf{r}', \omega). \end{aligned} \quad (A4)$$

The second term on the right-hand side of this equation vanishes because

$$\int d^3r' \chi_s(\mathbf{r}, \mathbf{r}', \omega) = 0, \quad (\text{A5})$$

which can easily be shown from the representation of χ_s in terms of the (orthonormal) Kohn-Sham orbitals [see Eq. (2) of Ref. 13]. This proves the sum rule for the exchange-correlation hole,

$$\int d^3r' n_{xc}(\mathbf{r}, \mathbf{r}') = -1, \quad (\text{A6})$$

for any approximation for the exchange-correlation kernel, as long as the density-density response function in this approximation can be written in the form of Eq. (A2). The sum rule for the correlation hole then follows from the fact that χ_λ to zeroth order in the coupling constant λ is just the Kohn-Sham response function χ_s , which leads to the exact exchange hole (which integrates to -1). From a physical perspective, Eq. (A5) follows from the fact that the density response $\delta n(\mathbf{r}, \omega) = \int d^3r' \chi_s(\mathbf{r}, \mathbf{r}', \omega) \delta v_s(\mathbf{r}', \omega)$ of non-interacting electrons to a potential $\delta v_s(\mathbf{r}', \omega) = c(\omega)$ must vanish.

APPENDIX B: RPA ON-TOP CORRELATION HOLE AND CUSP CONDITION FOR THE SPIN-UNPOLARIZED UNIFORM ELECTRON GAS

We focus first on the spin-unpolarized case ($\zeta=0$). The correlation part of the pair distribution function $g_\lambda(\mathbf{r}, \mathbf{r}')$ at interaction strength λ can be expressed in terms of density-density response functions:

$$g_{c,\lambda}(\mathbf{r}, \mathbf{r}') = \frac{1}{n(\mathbf{r})n(\mathbf{r}')} \left[-\frac{1}{\pi} \int_0^\infty d\omega \times \text{Im}[\chi_\lambda(\mathbf{r}, \mathbf{r}', \omega) - \chi_s(\mathbf{r}, \mathbf{r}', \omega)] \right]. \quad (\text{B1})$$

Here, $\chi_s(\mathbf{r}, \mathbf{r}', \omega)$ is the density-density response function of the noninteracting Kohn-Sham system, and $\chi_\lambda(\mathbf{r}, \mathbf{r}', \omega)$ is the corresponding response function for the interacting system at coupling strength λ .

In the RPA, the Fourier transform

$$\chi_\lambda^{unif,RPA}(q, \omega) = \int d^3(\mathbf{r} - \mathbf{r}') \exp[-i\mathbf{q} \cdot (\mathbf{r} - \mathbf{r}')] \times \chi_\lambda^{unif,RPA}(\mathbf{r} - \mathbf{r}', \omega) \quad (\text{B2})$$

of the density-density response function is given by

$$\chi_\lambda^{unif,RPA}(q, \omega) = \frac{\chi_s(k_F, q, \omega)}{1 - (4\pi\lambda/q^2)\chi_s(k_F, q, \omega)}, \quad (\text{B3})$$

where $\chi_s(k_F, q, \omega)$ is the Lindhard function, which depends parametrically on the Fermi wave number k_F . By Eq. (B1), the correlation part of the RPA pair distribution function of the uniform electron gas is then

$$g_{c,\lambda}^{unif,RPA}(r_s, u) = -\frac{18\pi^2\lambda}{k_F^6 u} \int_0^\infty dq \frac{\sin(qu)}{q} \int_0^\infty d\omega \times \text{Im} \left(\frac{\chi_s(k_F, q, \omega)^2}{1 - (4\pi\lambda/q^2)\chi_s(k_F, q, \omega)} \right). \quad (\text{B4})$$

By numerical integration of this expression, we have calculated the RPA pair distribution function at full coupling ($\lambda=1$). The frequency integration is most conveniently performed on the imaginary axis (see, e.g., Ref. 15). The results are shown for $r_s=2$ as the diamonds in Fig. 1.

For the on-top value, $g_c^{unif,RPA}(r_s, \zeta=0, u=0) = g_{c,\lambda=1}^{unif,RPA}(r_s, \zeta=0, u=0)$, we fitted the numerical results to the form

$$g_c^{unif,RPA}(r_s, \zeta=0, u=0) = -\frac{cr_s + \alpha r_s^2 + \delta r_s^3}{1 + \beta r_s + \gamma r_s^2}, \quad (\text{B5})$$

where $c=0.7317$, $\alpha=0.89058$, $\delta=0.050420$, $\beta=1.50419$, and $\gamma=0.168970$. Here c is not a fit parameter, but arises from the small- r_s expansion of Eq. (3.9) of Ref. 55.

Integrating Eq. (B5) over r_s , we obtain

$$\bar{g}_c^{unif,RPA}(r_s, \zeta=0, u=0) = \frac{1}{r_s} \int_0^{r_s} dr'_s \times g_c^{unif,RPA}(r'_s, \zeta=0, u=0) = -\frac{1}{r_s} F(r_s), \quad (\text{B6})$$

where

$$F(r_s) = 0.14920r_s^2 + 2.61428r_s + 24.95026 - 10.35413 \ln(1 + 1.50419r_s + 0.16897r_s^2) + 10.28879 \ln\left(\frac{r_s + 0.72362}{r_s + 8.17849}\right). \quad (\text{B7})$$

To obtain the RPA pair correlation function for arbitrary spin polarization ζ , one has to make the replacement

$$\chi_s(k_F, q, \omega) \rightarrow \frac{1}{2} [\chi_s(k_F(1+\zeta)^{1/3}, q, \omega) + \chi_s(k_F(1-\zeta)^{1/3}, q, \omega)] \quad (\text{B8})$$

in Eq. (B4). Making use of the explicit form of the Lindhard function (see, e.g., Ref. 57), one can deduce the spin scaling relationship

$$g_c^{unif,RPA}(r_s, \zeta=1, u=0) = 2g_c^{unif,RPA}(r_s/2^{4/3}, \zeta=0, u=0) \quad (\text{B9})$$

by appropriate substitution of the integration variables. For the coupling-constant average, one then obtains

$$\bar{g}_c^{unif,RPA}(r_s, \zeta=1, u=0) = -\frac{2}{r_s/2^{4/3}} F(r_s/2^{4/3}). \quad (\text{B10})$$

The proof of the RPA cusp condition for arbitrary spin polarization follows the lines of the original proof for $\zeta=0$ of Ref. 47. The cusp is related to the structure factor $S_\lambda(q)$ by

$$\left. \frac{dg_\lambda^{unif}}{du} \right|_{u=0} = \frac{3\pi}{8k_F^3} \lim_{q \rightarrow \infty} \{q^4[1 - S_\lambda(q)]\}. \quad (\text{B11})$$

In the RPA, the structure factor for arbitrary spin polarization ζ is given by

$$S_\lambda^{RPA}(q) - 1 = -1 - \frac{3q^2}{4k_F^3} \int_0^\infty d\omega \times \text{Im} \left[\left(1 - \frac{2\pi\lambda}{q^2} [\chi_s(k_F(1+\zeta)^{1/3}, q, \omega) + \chi_s(k_F(1-\zeta)^{1/3}, q, \omega)] \right)^{-1} \right]. \quad (\text{B12})$$

The integrand is nonzero only for those frequencies for which at least one of the two response functions has a non-

vanishing imaginary part. For large q , this is the case only if at least one of the two following conditions is satisfied for $0 \leq \zeta \leq 1$:

$$\frac{q^2}{2} - k_F q (1 + \zeta)^{1/3} \leq \omega \leq \frac{q^2}{2} + k_F q (1 + \zeta)^{1/3}, \quad (\text{B13})$$

$$\frac{q^2}{2} - k_F q (1 - \zeta)^{1/3} \leq \omega \leq \frac{q^2}{2} + k_F q (1 - \zeta)^{1/3}. \quad (\text{B14})$$

The frequency integral can then be split into three integrals, one for which both of the above conditions are satisfied simultaneously, and two for which only one of the conditions is true. For large q , the integrands of these integrals can be expanded in a power series in $1/q^2$ and the frequency integrals up to order $1/q^4$ can be performed. The final result for the structure factor in the RPA for large q is then

$$S_\lambda^{RPA}(q) - 1 = -\frac{8k_F^3\lambda}{3\pi q^4} + O(1/q^6), \quad (\text{B15})$$

independent of ζ . Insertion into Eq. (B11) then leads to Eq. (23).

*Present address: Department of Theoretical Physics 1, Lund University, Sölvegatan 14 A, S-22362 Lund, Sweden.

¹P. Hohenberg and W. Kohn, Phys. Rev. **136**, B864 (1964).

²W. Kohn and L.J. Sham, Phys. Rev. **140**, A1133 (1965).

³J.P. Perdew, K. Burke, and M. Ernzerhof, Phys. Rev. Lett. **77**, 3865 (1996); **78**, 1396(E) (1997).

⁴L.J. Sham and M. Schlüter, Phys. Rev. Lett. **51**, 1888 (1983).

⁵M.E. Casida, Phys. Rev. A **51**, 2005 (1995).

⁶S. Kurth, in *Electron Correlations and Materials Properties*, edited by A. Gonis, N. Kioussis, and M. Ciftan (Kluwer Academic/Plenum, New York, 1999).

⁷E. Engel and R.M. Dreizler, J. Comput. Chem. **20**, 31 (1999).

⁸A.D. Becke, J. Chem. Phys. **98**, 5648 (1993).

⁹J.P. Perdew, M. Ernzerhof, and K. Burke, J. Chem. Phys. **105**, 9982 (1996).

¹⁰J.P. Perdew, S. Kurth, A. Zupan, and P. Blaha, Phys. Rev. Lett. **82**, 2544 (1999); **82**, 5179(E) (1999).

¹¹S. Kurth, J.P. Perdew, and P. Blaha, Int. J. Quantum Chem. **75**, 889 (1999).

¹²M. Seidl, J. P. Perdew, and S. Kurth, Phys. Rev. Lett. (to be published).

¹³S. Kurth and J.P. Perdew, Phys. Rev. B **59**, 10461 (1999); **60**, 11212(E) (1999).

¹⁴P. Nozières and D. Pines, Phys. Rev. **111**, 442 (1958).

¹⁵D. Pines, *Elementary Excitations in Solids* (Benjamin, New York, 1964).

¹⁶U. von Barth and L. Hedin, J. Phys. C **5**, 1629 (1972).

¹⁷D.C. Langreth and J.P. Perdew, Phys. Rev. B **15**, 2884 (1977).

¹⁸D.C. Langreth and J.P. Perdew, Phys. Rev. B **21**, 5469 (1980).

¹⁹K.S. Singwi, M.P. Tosi, R.H. Land, and A. Sjölander, Phys. Rev. **176**, 589 (1968).

²⁰J.P. Perdew and A. Zunger, Phys. Rev. B **23**, 5048 (1981).

²¹J.P. Perdew and Y. Wang, Phys. Rev. B **45**, 13244 (1992).

²²G. Ortiz, M. Harris, and P. Ballone, Phys. Rev. Lett. **82**, 5317 (1999).

²³B.J. Alder, D.M. Ceperley, and E.L. Pollock, Int. J. Quantum

Chem., Quantum Chem. Symp. **16**, 49 (1982).

²⁴K. Moulouopoulos and N.W. Ashcroft, Phys. Rev. B **45**, 11518 (1992).

²⁵D.J.W. Geldart and M. Rasolt, Phys. Rev. B **13**, 1477 (1976).

²⁶J.M. Pitarke and A.G. Eguiluz, Phys. Rev. B **57**, 6329 (1998).

²⁷J.M. Pitarke and A.G. Eguiluz (private communication).

²⁸J. F. Dobson (private communication); J. F. Dobson and J. Wang (unpublished).

²⁹Z. Yan, J.P. Perdew, S. Kurth, C. Fiolhais, and L. Almeida, Phys. Rev. B **61**, 2595 (2000).

³⁰P.G. Reinhard, Phys. Lett. A **169**, 281 (1992).

³¹C. Guet and S.A. Blundell, Surf. Rev. Lett. **3**, 395 (1996).

³²F. Catara, G. Piccitto, M. Sambataro, and N. Van Giai, Phys. Rev. B **54**, 17536 (1996).

³³T. Kotani, J. Phys.: Condens. Matter **10**, 9241 (1998).

³⁴A.G. Eguiluz (private communication).

³⁵R. J. Bartlett (private communication).

³⁶N. Oliphant and R.J. Bartlett, J. Chem. Phys. **100**, 6550 (1994).

³⁷F. Furche (private communication). Filipp Furche recently sent us his preliminary results for the RPA+ atomization energies of small molecules. He found that large basis sets are needed to describe the deep cusp in the RPA correlation hole.

³⁸F. Haase and R. Ahlrichs, J. Comput. Chem. **14**, 907 (1993).

³⁹D.C. Langreth and M.J. Mehl, Phys. Rev. B **28**, 1809 (1983).

⁴⁰A.D. Becke, Phys. Rev. A **38**, 3098 (1988).

⁴¹K. Burke, J.P. Perdew, and M. Ernzerhof, J. Chem. Phys. **109**, 3760 (1998).

⁴²J.P. Perdew, Int. J. Quantum Chem., Quantum Chem. Symp. **27**, 93 (1993).

⁴³J.P. Perdew, K. Burke, and Y. Wang, Phys. Rev. B **54**, 16533 (1996); **57**, 14999(E) (1998).

⁴⁴J.P. Perdew, Phys. Rev. B **33**, 8822 (1986); **34**, 7406(E) (1986).

⁴⁵J.P. Perdew and Y. Wang, Phys. Rev. B **46**, 12947 (1992); **56**, 7018(E) (1997). See also Ref. 49, which shows that this parametrization is valid for $0.1 \leq r_s \leq 10$, and improves its decomposition into parallel- and antiparallel-spin contributions.

- ⁴⁶A.K. Rajagopal, J.C. Kimball, and M. Banerjee, *Phys. Rev. B* **18**, 2339 (1978).
- ⁴⁷J.C. Kimball, *Phys. Rev. A* **7**, 1648 (1973).
- ⁴⁸H.K. Schweng, H.M. Böhm, A. Schinner, and W. Macke, *Phys. Rev. B* **44**, 13 291 (1991).
- ⁴⁹K. Schmidt, S. Kurth, J. Tao, and J.P. Perdew, *Phys. Rev. B* (to be published).
- ⁵⁰A. Görling and M. Levy, *Phys. Rev. B* **47**, 13 105 (1993).
- ⁵¹M. Ernzerhof, *Chem. Phys. Lett.* **263**, 499 (1996).
- ⁵²M. Lein, E.K.U. Gross, and J.P. Perdew, *Phys. Rev. B* (to be published).
- ⁵³J. Harris and R.O. Jones, *J. Phys. F: Met. Phys.* **4**, 1170 (1974).
- ⁵⁴J.P. Perdew, H.Q. Tran, and E.D. Smith, *Phys. Rev. B* **42**, 11 627 (1990).
- ⁵⁵D.J.W. Geldart, *Can. J. Phys.* **45**, 3139 (1967).
- ⁵⁶E.K.U. Gross and W. Kohn, *Adv. Quantum Chem.* **21**, 255 (1990).
- ⁵⁷E.K.U. Gross, E. Runge, and O. Heinonen, *Many-Particle Theory* (Hilger, Bristol, 1991).
- ⁵⁸J.D. Talman and W.F. Shadwick, *Phys. Rev. A* **14**, 36 (1976).
- ⁵⁹L. Pollack and J.P. Perdew, *J. Phys.: Condens. Matter* **12**, 1239 (2000).
- ⁶⁰R.D. Amos, I.L. Alberts, J.S. Andrews, S.M. Colwell, N.C. Handy, D. Jayatilaka, P.J. Knowles, R. Kobayashi, G. J. Lamming, A.M. Lee, P.E. Maslen, C.W. Murray, P. Palmieri, J.E. Rice, J. Sanz, E.D. Simandiras, A.J. Stone, M.-D. Su, and D.J. Tozer. *CADPAC6: The Cambridge Analytical Derivatives Package Issue 6.0* Cambridge (1995).